Applied Catalysis B: Environmental 190 (2016) 137–146

Contents lists available at ScienceDirect

Applied Catalysis B: Environmental

journal homepage: www.elsevier.com/locate/apcatb

Equilibrium potassium coverage and its effect on a Ni tar reforming catalyst in alkali- and sulfur-laden biomass gasification gases

Pouya H. Moud [a,*], Klas J. Andersson [b], Roberto Lanza [a], Klas Engvall [a]

[a] KTH Royal Institute of Technology, School of Chemical Science and Engineering, Department of Chemical Engineering and Technology, SE-100 44 Stockholm, Sweden
[b] Haldor Topsoe A/S, Haldor Topsøes Allé 1, DK-2800 Kongens Lyngby, Denmark

ARTICLE INFO

Article history:
Received 22 December 2015
Received in revised form 29 February 2016
Accepted 4 March 2016
Available online 5 March 2016

Keywords:
Tar reforming
Biomass gasification
Ni-based catalyst
Potassium
Sulfur

ABSTRACT

Biomass conversion to syngas via gasification produces certain levels of gaseous by-products, such as tar and inorganic impurities (sulfur, potassium, phosphorus etc.). Nickel, a commonly used catalyst for hydrocarbon steam reforming, suffers reduced reforming activity by small amounts of sulfur (S) or potassium (K), while resistance against deleterious carbon whisker formation increases. Nevertheless, the combined effect of biomass derived gas phase alkali at varying concentrations together with sulfur on tar reforming catalyst performance under realistic steady-state conditions is largely unknown. Prior to this study, a methodology to monitor these effects by precise K dosing as well as K co-dosing with S was successfully developed. A setup consisting of a 5 kW biomass fed atmospheric bubbling fluidized bed gasifier, a high temperature hot gas ceramic filter, and a catalytic reactor operating at 800 °C were used in the experiments. Within the current study, two test periods were conducted, including 30 h with 1 ppmv potassium chloride (KCl) dosing followed by 6 h without KCl dosing. Besides an essentially carbon-free operation, it can be concluded that although K, above a certain threshold surface concentration, is known to block active Ni sites and decrease activity in traditional steam reforming, it appears to lower the surface S coverage (θ_s) at active Ni sites. This reduction in θ_s increases the conversion of methane and aromatics in tar reforming application, which is most likely related to K-induced softening of the S—Ni bond. The K-modified support surface may also contribute to the significant increase in reactivity towards tar molecules. In addition, previously unknown relevant concentrations of K during realistic operating conditions on typical Ni-based reforming catalysts are extrapolated to lie below 100 μg K/m^2, a conclusion based on the 10–40 μg K/m^2 equilibrium coverages observed for the Ni/$MgAl_2O_4$ catalyst in the present study.

1. Introduction

Biomass utilization is recognized as one realizable solution with high potential for the future to meet our current energy and environmental challenges [1–3]. The main drivers for the increased interest towards biomass are related to sustainable energy issues, as well as to its abundance and the potential of reducing the emission of greenhouse gases [1,2,4,5]. Among different thermochemical pathways for biomass conversion, gasification has attracted the most attention due to its high conversion efficiency and its versatility in accepting a wide range of biomass feedstocks to produce an intermediate syngas suitable for further upgrading to various high-value end products [4,6,7].

The producer gas or fuel gas produced must be cleaned and suitable for downstream devices [8,9]. High content of tar, *i.e.* polyaromatic hydrocarbon byproducts from the biomass gasification, can lead to many operational difficulties such as condensation at temperatures below 350–400 °C, plugging and corrosion of pipes and equipment, as well as formation of carbon deposits on catalysts in downstream processing [3,10]. The level of tar, produced in a gasification process, is dependent on the type of gasifier. According to Milne et al. [11], a very crude generalization of tar level for different gasifiers is in the range of 1–100 g/Nm^3, where in general terms, downdraft gasifiers are considered as the cleanest, updraft gasifiers the dirtiest and fluidized bed gasifiers are in the lower intermediate range [11]. For a given gasifier, the level of tar is dependent on the process conditions, such as the biomass type and its particle size

* Corresponding author.
E-mail addresses: pouyahm@kth.se, pooya.ha@gmail.com (P.H. Moud).

http://dx.doi.org/10.1016/j.apcatb.2016.03.007
0926-3373/

distribution, and on the operating conditions of the reactor, including temperature, gasifying agent (air, steam, steam-O_2), and other parameters related to the selected technology. Hot gas conditioning methods for tar elimination are usually preferred compared to other methods, since they eliminate tars by converting them into useful permanent gas components and thus retaining the chemical energy in the product gas, as well as avoiding treatment of an additional waste stream, as for wet methods [12]. An attractive option, among hot gas conditioning methods, is catalytic steam reforming using a nickel-based catalyst. This method offers several advantages, such as high tar conversion, thus also increased syngas yield, and thermal integration of the process to the gasifier exit temperature [3,12,13]. Several different types of Ni-based catalysts have been tested and found to be cost-effective for tar reforming application in comparison to other types of catalyst [3,13–17].

In tar reforming applications, a Ni-based catalyst is exposed to a number of inorganic trace components such as alkali, sulfur, phosphor and chloride species, as well as other trace elements [8,15,18,19]. The level of these inorganic impurities in the biomass gasification gas depends on several parameters such as the gasification technology employed, the process conditions of the given gasifier, the type of biomass and the choice of technology for gas cleaning upstream of the catalytic reactor such as if a hot gas filter being used for particulate removal [8,20,21]. The impurity level of S, Cl, and N compounds in the gas phase seems to be well correlated with the biomass composition and gasification conditions. The levels are in general between 20 and 200 ppm volumetric (ppmv) on dry gas basis (db) for both S (mainly H_2S) and Cl (mainly HCl) compounds [15,18], and 500–3000 ppmv (db) for NH_3, in case of woody biomass [22]. The large part of the alkali is retained in the gasifier ash, and in case of fluid bed gasifiers, also in the bed solids. Typical gas phase K-species levels are around 0.01–5 ppmv (db), with one case reported as high as 25–30 ppmv [8,18,23–25].

Small amounts of sulfur and potassium influence the activity of the catalyst. For instance, as previously shown [26,27], the potassium in K-promoted nickel catalysts increases the resistance to carbon formation. However, it is also shown that potassium, above a certain threshold concentration, decreases the steam reforming activity [26,28] as well as the hydrogenation activity [29]. Sulfur, a known and severe poison for Ni steam reforming catalyst, tends to retard the formation of whisker carbon above certain coverages, due to blockage of C nucleation sites [26,28,30,31]. Optimally, a catalyst promoted with sulfur and potassium will just have enough additives to block coke formation and still proceed at sufficient reaction rates [32]. Cl and NH_3 do not seem to affect the reforming performance of the Ni catalyst [33,34].

Co-adsorption of K and S on Ni has been investigated in several surface science related studies. For instance, in a study performed by Chen and Shiue [35], it was proposed that the adsorbing ability of sulfur compound on nickel surfaces decreases for the potassium promoted nickel, as the surface concentration of potassium increases. They hypothesized this to be the result of electron transfer to nickel by adsorbed K, inhibiting the formation of nickel sulfide. Politano et al. [36] observed a Ni—O bond weakening, during co-adsorption of K and O, in studies of the related K-O/Ni system. As it would also be expected for the similar K-S/Ni system, it was argued that electron donation from K to the O/Ni system results in a filling of Ni—O anti-bonding states. The observed Ni—O bond weakening, upon K co-adsorption, confirmed prior DFT results regarding K co-adsorption induced metal-oxygen bond weakening [37]. In another study by Ferrandon et al. [38] on Rh/La-Al_2O_3 for hydrogenation of benzene, it was suggested that besides inhibition of coke formation, the improvement in sulfur tolerance of the catalyst could be related to alkali blocking part of the catalyst and thus hindering the adsorption of H_2S and thiophene [38]. Papageorgopoulos et al. [39], established that K interacted strongly with S at a Ni surface. The formation of a KS compound was observed for high S coverages, *i.e.* S coverages higher than 0.5 monolayer (ML), and was taken as evidence for a K-induced S—Ni bond weakening. Similarly, in studies by Blaszczyszyn et al. [40,41], pre-deposited S on a Ni (100) surface was found to drastically increase the binding energy of potassium. They speculated that the increased K binding energy could be due to an increase in the work function of the clean nickel by sulfur, enhancing the ionic adsorption of potassium on the S/Ni surface.

Evidently, both negative and positive sulfur and potassium adsorption effects have been documented. The combined effect of potassium and sulfur on a Ni-based catalyst under steady-state tar (steam) reforming process conditions has not yet been clarified. There are only very few studies of the effect of alkali on tar reforming catalysts [34,42–44]. A limitation in all these studies is the method used to investigate the influence of K on the catalyst, which is different from actual mechanisms of potassium transport, deposition and equilibration on the catalyst [34]. In addition, few of these studies were performed under exposure to real producer gas from biomass [44], as well as none were investigated under realistic steady-state conditions [34,42–44]. In a study by Li et al. [42], pre-exposure of alkali salt vapors to a monolithic Ni-based catalyst, resulted in loss of surface area and deactivation of the reforming reaction. Albertazzi et al. [44] and Einvall et al. [43] observed a recovered or only a minor loss in reforming activity after pre-deposition of K species on the Ni catalysts. The reason for both phenomena was related to a cleaning effect of steam (alkali volatilization) during activity tests and under reforming condition of a real producer gas.

In our previous study [45], we developed a methodology to enable the investigation of combined effects of biomass-derived impurities in gas phase under realistic steady-state conditions on a typical tar (steam) reforming catalyst. Aging of the catalyst resulted in stable BET and nickel surface areas. Pre-sulfidation of the catalyst caused an isolation of K effects on catalyst performance by removing the transient in activity of the catalyst due to change in S coverage. The pretreated catalyst exposure tests were carried out with real producer gas. However, since time on stream was rather short, the results were inconclusive as to whether K has any impact on catalyst activity. Another observation was a significant slowdown in K uptake with increased hydrogen sulfide concentration in the gas, an effect discussed in terms of K preferential adsorption sites and possible spill-over phenomena. In the present study, we continue with a longer exposure time to determine the K equilibrium coverages on the catalyst, as well as its effect on the catalyst performance. The K and S concentration profile in the catalytic bed is also investigated to study the effect of K on the S—Ni system. In addition, the early stage of alkali removal from the catalytic bed and its effect on reforming activity, while reducing the alkali content in the gas phase were investigated.

2. Experimental

2.1. Experimental setup

All experiments were performed in a gasification system, consisting of a 5 kW pine pellet fed atmospheric bubbling fluidized bed gasifier, a high temperature hot gas ceramic filter, a fixed bed catalytic reactor, a cleaning section, an analytic section and an aerosol generator setup. The hot gas filter is used to remove particulates. Alkali metal compounds were produced and dosed into the dust-free raw producer gas through a setup consisting of two main parts: an aerosol generator (Constant Output Atomizer model 3076, TSI Inc.) and a homemade diffusion dryer (similar to model 3063, TSI Inc.). Fig. 1 shows the schematic of the experimental setup used in

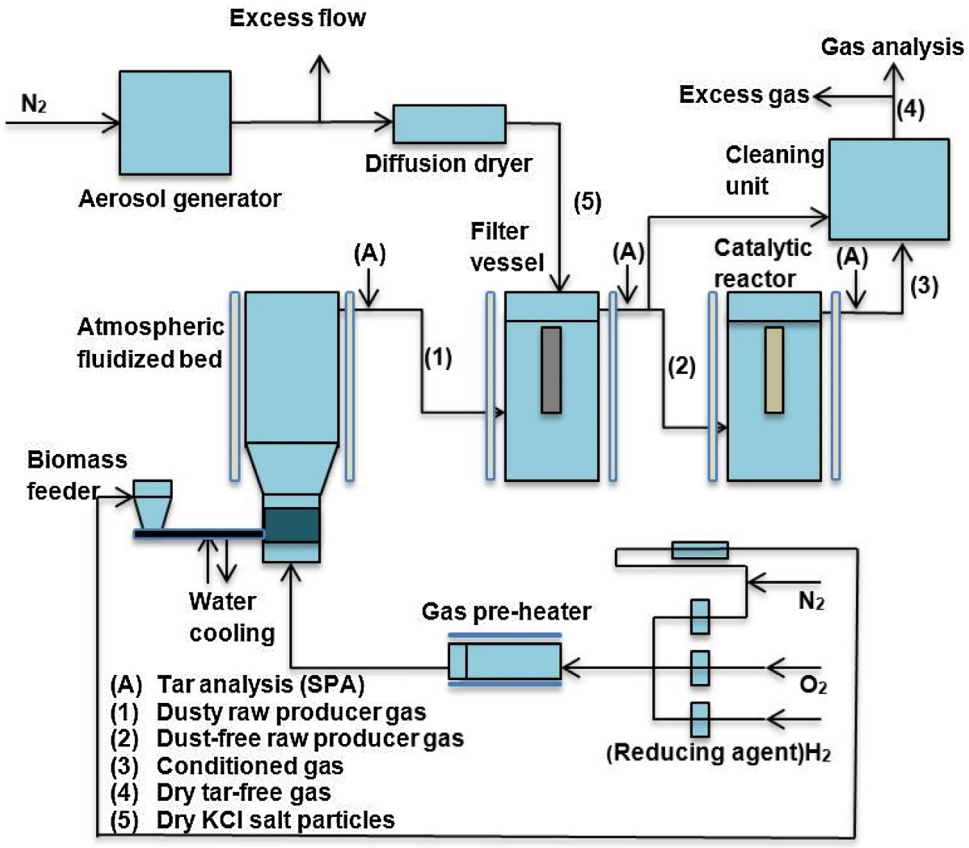

Fig. 1. Schematic view of the experimental setup adapted from Moud et al. [45].

the tests. The detailed description of the setup is found elsewhere [45].

2.2. Materials and methods

2.2.1. Materials

Pine pellets, in the size range of 1.5–2 mm, were used as the feedstock. The properties of the used biomass is found elsewhere [45]. The bed material used in the fluidized bed was dense α-alumina (350 g) with a particle size of 63–125 μm and density of 3960 kg/m^3. Nitrogen was used as fluidization medium, while the oxidizing agent was pure oxygen. The steam reforming catalyst was a Ni/$MgAl_2O_4$ catalyst (Haldor Topsøe A/S, HT-25934). Inert silica-free filler (Vereinigte Füllkörper-Fabriken, DURANIT® Inert Balls D99 with the size of 1/8″) was mixed with the studied catalyst in the catalytic bed.

2.2.2. Tar and gas analysis

The composition of the dry tar-free gas was determined with a micro-GC (Thermo Scientific, C2V-200). Tar samples were collected and analyzed using the solid phase adsorption (SPA) method [46]. A gas sample of 100 ml was manually taken through an amino sorbent. Later the solid phase extraction tube was eluted, using dichloromethane and dichloromethane/acetonitrile (1:1), to obtain an aromatic fraction and phenol fraction. The collected samples were analyzed, using a gas chromatograph (Varian CP 3800). The hydrogen sulfide, originating from biomass, was measured with an optical feedback cavity enhanced absorption spectrometer (OFCEAS). Two samples of dry tar-free gas were collected during the biomass gasification in gas bags and sent to SP Technical Research Institute of Sweden for analysis. The analysis was based on laser IR spectrometry.

2.2.3. Catalyst activity

The catalyst activity is determined by evaluation of the conversion (X_i) of methane, naphthalene, and C_{10+}, from data collected at two different sample points, before and after the catalytic reactor via micro-GC and SPA analyses. The conversion is calculated according to Eq. (1):

$$X_i = 1 - \frac{N_{i,\text{out}}}{N_{i,\text{in}}} \quad (1)$$

where N_i is the number of moles of species *i*.

2.2.4. Thermodynamic calculation

Thermodynamic equilibrium calculations were performed using the program NASA CEA Code [47] to determine the most abundant equilibrium K species in the gas phase. The calculations are based on real producer gas compositions with the addition of different gas phase alkali concentrations. Calculation of the water content is based on the water gas shift equilibrium (WGS), as shown in Eqs. (2) and (3):

$$CO + H_2O \leftrightarrow CO_2 + H_2 \quad (2)$$

$$K_{eq} = \frac{[CO_2][H_2]}{[CO][H_2O]} \quad (3)$$

2.2.5. Catalyst characterization

To determine the total sulfur and carbon content on the catalyst surface, chemical analysis of the fresh and used catalyst were performed by LECO, CS230 series and ELTRA, CS-2000 series instruments. The K content of the catalyst was measured using atomic absorption spectrometry (AAS), (PerkinElmer, model 1100 B AAS analyzer). Samples (200–400 mg) for AAS analysis were dissolved in boiling HNO_3 in a standard flask and afterwards diluted with

distilled water to a known volume. The surface area measurements were performed and calculated by N_2 adsorption/desorption (Micromeritics, ASAP 2000) and Brunauer–Emmett–Teller (BET) method with data collected at relative pressures between 0.06 and 0.2. The samples were outgassed under vacuum and temperature of 250 °C for 4 h prior to analysis. Data were collected at liquid nitrogen boiling temperature (77 K).

2.2.6. Alkali characterization

It is crucial to perform the alkali aerosol dosing under realistic conditions. A number of characterization tests were carried out in the previous study [45] to prove that introduction of alkali was done under a well-controlled and repeatable conditions for all the experiments. Alkali salt particle size distribution were measured using a scanning mobility particle sizer (SMPS), (TSI Inc., model 3936). The dosed alkali aerosol mass concentration was determined by a different set of experiments. The prepared alkali solution at each concentration corresponds to a specific gas phase ppmv level, assuming all alkali evaporates into the gas phase. The detailed calibration description of the aerosol generator outlet concentration, as well as methods used for alkali aerosol particle size distribution and content measurement in the gas phase, is described in the previous study [45].

2.2.7. H_2S chemisorption

Hydrogen sulfide chemisorbs dissociatively on nickel. The actual sulfur coverage, θ_s, is represented by a linear isobar expression [48]:

$$\theta_s = 1.45 - 9.53 \times 10^{-5} T + 4.17 \times 10^{-5} T \ln\left(P_{H_2S}/P_{H_2}\right) \quad (4)$$

Eq. (4) is less accurate for low sulfur coverages and θ_s close to 1 (*i.e.*, monolayer saturation, ca 0.5 ML S, see Ref. [26] and references therein).

2.2.8. System pre-conditioning and activity tests

To eliminate transient effects in catalytic performance, due to initial catalyst sintering and sulfidation, a pretreatment step was performed for 5 h of accelerated aging at high temperature (920 °C), $H_2O/H_2 = 10$ and a sulfur coverage equilibration by pre-sulfidation at 800 °C for 4 h. The calculated sulfur coverage of the catalyst, during sulfidation, was approximately 0.97. A detailed description of the pre-treatment procedure is explained elsewhere [45]. One of the observations after the pretreatment step in the previous work was the significant increase in K content of the catalyst. It was argued, such phenomenon was most likely an effective vaporization of residual K, located on surfaces in the gasification setup upstream of the catalytic bed. The induced volatilization is related to high temperature and partial pressure of water used during the pre-aging process. Therefore, in the current study, a steam-cleaning procedure was introduced prior to the pretreatment step. In this step, the whole gasification setup was steam-cleaned with addition of 10 l/min steam at 900 °C for 12 h.

After steaming and pre-treatment of the catalyst, a series of tests, including a total of 36 h time on stream, were performed. This was achieved in nine consecutive tests, seven tests with 1 ppmv KCl dosing (Period 1) for 30 h followed by two tests with no KCl dosing (Period 2) for 6 h. The temperature of the gasifier and filter was 850 °C, while the catalytic bed temperature was kept at 800 °C, *i.e.* 50 °C lower than in the previous study [45]; all three vessels are heated externally. Compared to some of the earlier experiments, no additional H_2S was added to the dust-free raw producer gas during Period 1 & 2, since the desired sulfur coverage was achieved ($\theta_s = 0.97$) without the need of tailoring the sulfur chemical potential in the dust-free raw producer gas. After steam cleaning of the setup and prior to the pretreatment steps, the catalyst was reduced for 4 h in H_2 at 700 °C. A summary of operating and experimental conditions of the system is presented in Table 1.

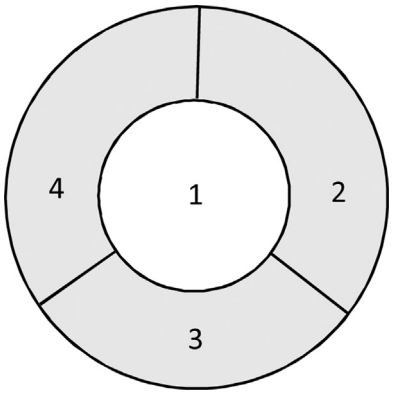

Fig. 2. Cross sectional area view of the catalytic bed and its different sampling zones.

The Ni-catalyst was crushed and sieved; 50 g of the 3–6 mm sieved fraction were used in the tests mixed with 50 g of inert filler. The loaded catalyst volume and total gas flow rate were selected to obtain partial hydrocarbon conversion. This was done in order to obtain an effective conversion range, enabling the comparison of catalyst activity at different conditions. Catalyst samples were collected in small amounts from the inlet of the catalytic reactor for characterization after cooling down in a nitrogen flow to ambient temperature every second or third test so that the change in catalyst amount, did not affect the tar reformer performance in a significant way. At the end of the series of tests, samples from different heights, through the bed, were taken to investigate the K and S concentration profile. This was done by emptying the reactor into a measuring plastic cup. The whole catalytic bed volume was around 55 ml. Samples were collected at approximately 0, 5, 10, 15, 20, and 25 mm axial distances by emptying the cup 10 ml at a time. Friction against the reactor wall, when emptying, may have transferred some material around during unload, but this should be less likely in the center zone of the bed. Consequently, to check the results for consistency, samples were collected from the central area of the bed, as well close to the wall, as shown in Fig. 2. Zone 1 represents the area around the center and zone 2, 3 and 4 represent the area near the reactor wall.

It is important to mention that after each test, the filter and the fluidized bed gasifier were cleaned thoroughly. The reason was that a gradual build-up of particulates over the filter normally results in tar reduction, as well as in cracking of heavier species to lighter ones [20,21]. Nemanova and Engvall [49] pointed out that due to char and ash accumulation in the gasifier over time, tar reduction is also initiated in the gasification bed [49]. In addition, the gradual build-up of particulates in the filter has a complex sorption effect on impurity levels [6,8,20,21], which is why KCl was added after the hot gas filter, in order to ensure constant dosing rates to the reactor.

3. Results

3.1. Speciation

Thermodynamic equilibrium calculations were performed in order to obtain a picture of the type of alkali compounds present in the produced gas stream after dosing KCl. The actual ratios of the potassium compounds depend on the biomass composition and gasification conditions, as mentioned earlier. In the previous study [45], the calculation showed that the gas phase potassium was mainly distributed between KCl, KOH and elemental K in the catalytic tar reformer. Addition of potassium chloride to the gas stream increased the content of relevant highly mobile potassium species. In the present study, the average wet gas composition at

Table 1
Summary of experimental and operating conditions of tests.

Total time on stream (ToS) (h)	36
N_2 flow rate (l/min)	11.4
O_2 flow rate (l/min)	0.9
Reactor temperature (°C)	800
H_2S concentration, biomass derived (ppmv)	15 ± 3
Steam-cleaning of the setup	12 h, 10 l/min steam, 900 °C
Pre-treatment step	
Cat. sulfidation	5 h of tailored H_2S/H_2 addition at 800 °C
Cat. aging	5 h of H2O/H2 addition at 920 °C for accelerated aging
$\frac{p_{H_2S}}{p_{H_2}}$	136 10^{-6}
Average biomass feed rate (g/min)	2.638
Average total inlet gas flow rate (Nl/min)	15.05
Average product gas yield (Nm^3/Kg fuel)	1.39
Average gas space velocity (Nm^3/Kgcat min)	0.31
Dosing KCl concentration (ppmv)	30 h ToS 1 ppmv (Period 1) 6 h ToS 0 ppmv (Period 2)
Initial catalyst amount (g)	50

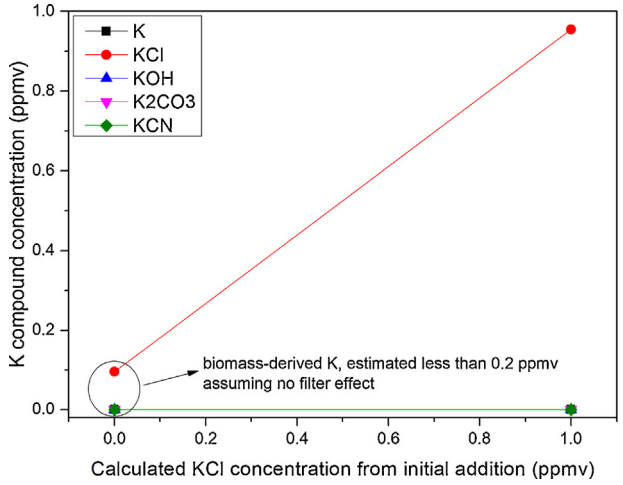

Fig. 3. Calculated potassium compounds concentration as a function of calculated KCl concentration from initial addition to dust-free raw producer gas. NH_3 and HCl are calculated to be approximately 400 and 30 ppmv respectively, T = 800 °C, biomass-derived K level is estimated less than 0.2 ppmv based on a comparison with Erbel et al. [23] study.

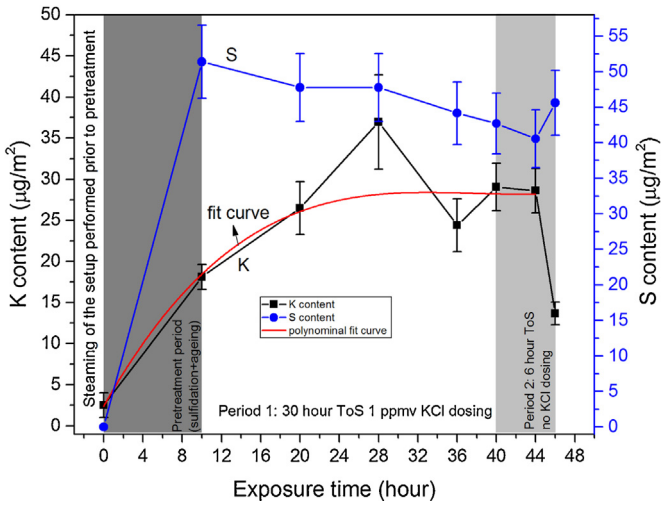

Fig. 4. Normalized sulfur and potassium content at the bed inlet vs exposure time. The fit curve only serves as a guide to the eye. The average BET surface area for samples taken during time on stream is 14.3 ± 1.6 m^2/g.

the catalytic reactor inlet is used for chemical equilibrium composition calculations at 0 and 1 ppmv KCl dosing concentration. The biomass-derived K in the gas is estimated to less than 0.2 ppmv [23], and based on the N and Cl content in the biomass, the levels of NH_3 and HCl are calculated to about 400 and 30 ppmv, respectively, assuming complete conversion to gas-phase species and no hot gas filter effects. This assumption is reasonable, since the H_2S concentration was calculated to 14 ppmv, based on the same assumption in our previous study [45], an estimation very close to the measured biomass derived H_2S concentration (15 ± 3 ppmv). According to Fig. 3, KCl is the most abundant K specie at 0 ppmv KCl dosing, considering less than 0.2 ppmv biomass-derived K in the gas. As the dosing concentration increases to 1 ppmv, the KCl concentration increase as well, confirming our previous results [45].

3.2. Catalyst characterization: potassium and sulfur content

Fig. 4 presents the normalized catalyst K and S content at the bed inlet, where exposure time is defined as the time for pretreatment plus the time on stream. Time on stream is the accumulated time the sample was exposed to dust-free raw producer gas from biomass, during Period 1 & 2. The K and S content of the exposed samples are normalized by the average BET surface area (14.3 ± 1.6 m^2/g) from all samples collected during time on stream. Data points at 0 h exposure time represent the characterization results of the fresh sample. An increase in K/average BET of the catalyst is observed after the pre-treatment step. This is most likely due to evaporation of K residuals in the system, subsequently deposited on the catalyst in the pretreatment step. Although the catalyst K level after pretreatment decreased, compared to when no steam cleaning was used in the previous study [45], the results show that despite the attempts, complete cleaning of the system from residual K was not achieved. Still, as shown in Fig. 4, the normalized K content increases with exposure time up to around 28 h. From 28 h up to 40 h, the K content seems to fluctuate around the same value reached already after 20 h. This is a clear indication that the potassium content reaches a plateau, as illustrated by the guide-to-the-eye curve in Fig. 4. Subsequently, after 6 h with no KCl dosing (Period 2), the potassium content of the catalyst at the bed inlet decreases to values lower than 15 μg/m^2. The sulfur content increases during the pretreatment period to 51 μg/m^2 due to the pre-sulfidation procedure. The S content thereafter gradually decreases with time on stream (Period 1) down to approximately 40 μg/m^2. Normalized S content appears to increase in the last 2 h of Period 2, simultaneously as the K content decreases.

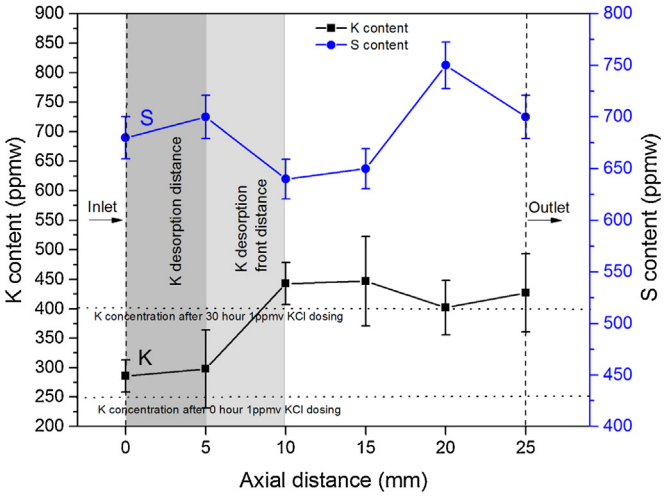

Fig. 5. Sulfur and potassium content profile in the catalytic bed at the end of Period 2. The average BET surface area for samples taken at different axial bed distances is $13.7 \pm 1.6\ m^2/g$.

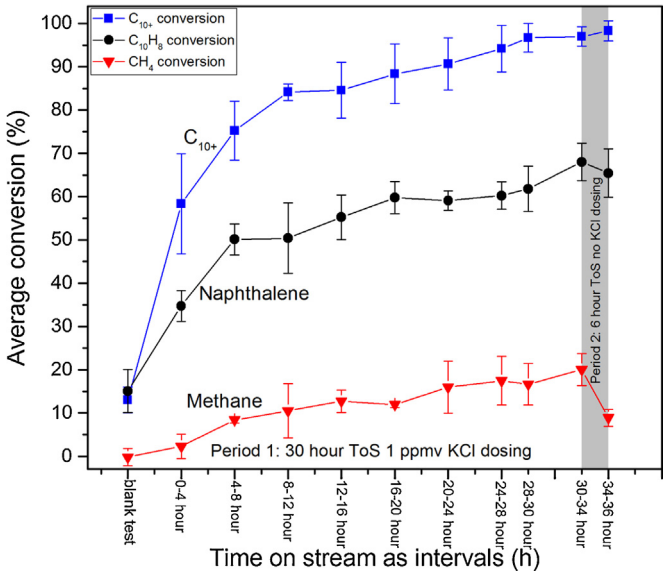

Fig. 6. Average methane, naphthalene and C_{10+} conversion versus time on stream as intervals for period 1&2. The catalytic reactor temperature is 800 °C. Blank tests were performed in the empty reactor.

3.3. Sulfur and potassium profile in the catalytic bed

Fig. 5 shows the K and S concentration profile in the catalyst bed versus the axial bed distance. Samples were taken from different bed heights after 36 h, *i.e.* at the end of the 6 h exposure without KCl dosing (Period 2). Each K data point in Fig. 5 represents an average of two measurements from zone 1 around the center (see Fig. 2). Average K measurements from zones 2, 3, and 4 near the reactor wall were also performed to investigate possible K concentration differences in the radial direction, but no obvious differences were observed. Therefore, only the K profile of the catalytic bed center is displayed. As displayed in Fig. 5, a K migration from the bed inlet has occurred with a desorption front located somewhere between the sample points at 5 and 10 mm from the inlet of the catalytic bed. This K desorption is also demonstrated when comparing to dashed horizontal lines, representing the average bed inlet K concentration at 0 and 30 h ToS from Fig. 4. Beyond the K desorption front, the K content exhibits an initial increase, but is, in general, quite stable around the same K concentration as that of the samples at the bed inlet after 30 h ToS (Period 1), *i.e.* before stopping the KCl addition. A clear trend with respect to S content throughout the bed is more difficult to discern. However, judging from what appears as an inverse relationship between S and K concentration, the two species seem to anti-correlate.

3.4. Gas composition

Table 2 shows the average reactor inlet wet gas compositions of major and minor components as molar flow rates. The outlet average wet gas compositions are also shown at different time intervals. The total content of tar (excluding benzene) is less than 0.1% of the inlet molar flow rate to the catalytic reactor. The mass balance for C, H and O over the reactor, excluding tar content, is 0.91–1.01, proving an acceptable mass balance. The absolute standard deviations for the major and minor components at the reactor inlet are presented in parentheses in Table 2. The reason for the deviations is due to the gradual buildup of a filter cake over time, as discussed earlier. Errors induced by the tar sampling method also affected the tar measurement, which was considered when calculating the tar conversion.

Fig. 6 shows the methane, naphthalene, and C_{10+} conversions over time. C_{10+} components include 2-methylnaphthalene, 1-methylnaphthalene, biphenyl, acenaphthylene, acenaphthene,

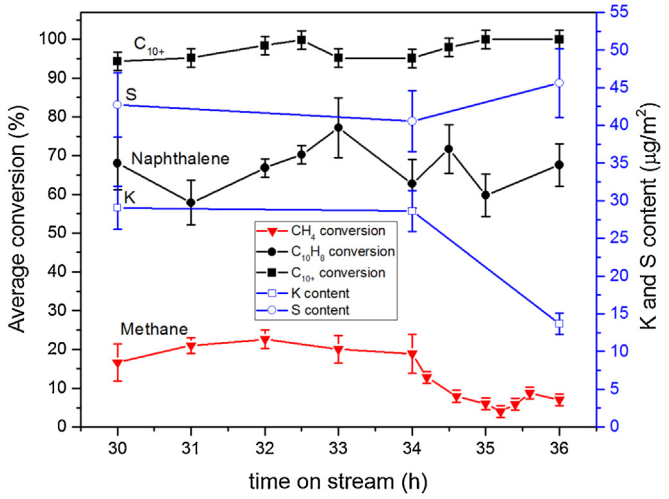

Fig. 7. Average methane and tar conversion, bed inlet S and K content versus time on stream for Period 2 with higher time resolution.

fluorene, phenanthrene, anthracene, fluoranthene and pyrene. Each conversion data point for naphthalene and tar components higher than naphthalene represents an average of six to eight samples over a time period of either two or four hours. Data points for methane represents an average of 12–16 samples over a time period of either two or four hours. Blank test data points represent the conversion occurring in the empty reactor. Methane conversion is almost zero while $C_{10}H_8$ and C_{10+} conversion is around 15%. A naphthalene conversion of around 20% was previously reported for empty reactor studies by Nemanova et al. [10] with the same setup, operating at 800 °C. It was concluded that thermal conversion was the reason for this reforming activity for naphthalene and tar in general [10]. There is a significant initial increase in conversion during the first 10–15 h time on stream for methane, naphthalene and C_{10+}. Subsequently, the catalyst reforming activity of methane, naphthalene and C_{10+} increases over time with a slower rate towards the end of Period 1.

Fig. 7 presents the Period 2 part of the previous Fig. 6 hydrocarbon conversion with higher time resolution. The measured bed

Table 2
Average molar flow rates in Period 1 and 2 before and after the catalytic reactor. Values inside the parentheses are calculated absolute standard deviations.

	Catalytic reactor inlet Period 1 & 2[d]	Catalytic reactor outlet					
		Period 1: 1 ppmv KCl dosing				Period 2: 0 ppmv KCl dosing	
Time on stream (hour)		0–10	10–18	18–26	26–30	30–34	34–36
Major components (mol/h)							
H_2O[a]	4.36 (0.36)[d]	4.27	3.94	4.71	4.60	4.48	5.00
CO_2	3.79 (0.17)	3.66	3.45	3.51	3.39	3.28	3.54
CH_4	2.65 (0.15)	2.32	2.33	2.31	2.25	2.21	2.29
CO	10.82(0.23)	10.73	11.10	10.73	10.86	10.96	10.28
H_2	12.22(0.37)	13.25	13.42	12.97	13.20	13.38	13.16
C_2H_4	0.65 (0.10)	0.35	0.35	0.34	0.29	0.28	0.28
N_2 (mol/h)	28.06						
total flow rate (mol/h)	62.58	62.67	62.67	62.66	62.68	62.67	62.65
Minor components tars, absolute values (g/Nm^3)							
Naphthalene $C_{10}H_8$	0.59(0.16)	0.29	0.27	0.29	0.25	0.20	0.18
Tar (excluding benzene)	1.15(0.29)	0.49	0.43	0.46	0.40	0.34	0.33
C_{10+}	0.25(0.11)	0.06	0.04	0.04	0.01	0.01	0.01
K and H_2S, absolute values (ppmv)							
KCl (from biomass)[b]	<0.2						
KCl (added)	1 (Period 1) 0 (Period 2)						
H_2S (from biomass)[c]	15 ± 3						

[a] Calculated using WGS equilibrium.
[b] Estimated based on a comparison with Erbel et al. [23] study (assuming no high T hot gas filtration effect).
[c] H_2S concentration measured, see Section 2.2.2.
[d] Values inside the parentheses are calculated absolute standard deviations.

inlet K and S concentrations on the catalyst are also plotted. After a three to four hour delay, following the replacement of the KCl solution in the aerosol generator to that of pure water, the potassium decreases and sulfur increases at the bed inlet. During this period of observed K and S changes, the methane conversion also decreases significantly, from approximately 19% to roughly 8%. Taking into account the standard deviations in tar measurement, no statistically significant changes in activity for naphthalene and C_{10+} are observed in Period 2.

4. Discussion

4.1. Potassium uptake/removal

Starting from approximately 17 μg K/m^2, for the pre-treated surfaces, and following the K content in the inlet of the catalytic bed over time (Fig. 4), a stable content of approximately 27 μg/m^2 is reached after 30 h time on stream. The observations in our previous study [45], implying a fairly slow approach to K-equilibrated surfaces, is confirmed by the longer exposure time, displaying stable content of K achieved on the catalyst surface. The K decrement to less than 15 μg/m^2 at the bed inlet in Period 2, shown in Fig. 4, is clearly due to the altered partial pressure of KCl in the gas phase, resulting in a change in potassium equilibrium surface coverage. In Campaign 3 of our previous study [45], the K content did not change significantly with time on stream during alkali dosing. This was most likely due to the lack of a steam-cleaning procedure for K removal in the gasification system, causing substantial uptake of K, originating from residuals in the system. On the basis of the results, obtained in the current study, it is clear that the K coverage results at the end of the different shorter campaigns in our prior study, as was also indicated, were not far from equilibrium. Combining all our results obtained, K equilibrium coverages on our Ni/$MgAl_2O_4$ catalyst is 10–40 μg K/m^2 under realistic steady-state tar reforming conditions. We extrapolate relevant K surface coverages under these conditions at temperatures ≥800 °C to be below 100 μg/m^2 for typical Ni (10 ± 5 wt-%) on high-temperature fired (20 ± 15 m^2 BET) alumina(te)-based (γ- and α-Al_2O_3, Mg- and Ca-aluminates) steam reforming catalysts.

Taking a closer look at the trends of S and K in Period 1 and 2 in Fig. 4, the gradual decrease of S in Period 1 and the sudden increase of S in Period 2 appear to be a primary effect of the K uptake and removal. In Campaign 3 of the previous study [45], the sulfur content did not change by time on stream. This result was most likely due to equilibrated K on the catalyst and no further uptake of K after the pretreatment as discussed earlier. There are different possibilities on why sulfur coverage changed over time in the present study. The H_2S/H_2 ratio is fixed during sulfidation in the pretreatment step and thus formed an S equilibrated catalytic reactor bed. Throughout steam reforming of tar, in combination with the water gas shift reaction, hydrogen molar flow increases throughout the bed. The hydrogen sulfide content is, on average, constant, assuming no slowly changing effect of the hot gas filter. Therefore, according to Eq. (4), a decreasing H_2S/H_2 ratio in the reactor over time could lower the sulfur coverage on Ni. However, the observed changes in S concentration (Fig. 4) and changes in H_2 production at different time intervals (Table 2) do not agree with sulfur coverage changes, calculated with Eq. (4), as no significant change is observed neither for the reactor inlet nor the exit H_2 concentration over the 36 test hours.

According to the observed results, the strongest cause for the observed S and K relation in this study is believed to be related to increased Ni sulfur resistivity due to K adsorption. As mentioned earlier in the introduction, K weakens the bond for Ni—O when the electronic field of K shifting electronic states, resulting in a donation of electron density to anti-bonding states [36]. The chemical bonding of S and O to nickel should not be too dissimilar and therefore the effect of K donating electron density to anti-bonding states of metal-oxygen and metal-sulfur bonds is expected to be similar. Another more direct mechanism for S—Ni bond weakening is the bond-order conservation model, where the strong K-S attractive interaction is expected to result in a weakening of the S—Ni bond. Either scenario above will result in a weakened S-bonding to the Ni surface by a certain degree of K co-adsorption, result-

ing in S-poisoning being drastically reduced. As the S—Ni bonding weakens, the S speciation equilibrium will shift toward the gas-phase, as well as probably result in an increase in surface S reactivity toward hydrogenation and oxygenation reactions. In the K adsorption curves in our previous study [45], higher sulfur concentration in the gas phase was found to retard the K uptake [45]. This does not contradict a significant K co-adsorption with S on Ni, but may rather reflect a reduced K sticking coefficient at an increased sulfur spillover to the support, which may result in a reduction of the ability of K to titrate support hydroxyl sites and form strong Al—O(H)—K bonds [50,51]. Support hydroxyl sites may constitute the main fraction of K adsorption sites on the catalyst. Therefore, based on prior temperature dependent alumina dehydroxylation studies [52,53], and relative differences in surface hydroxyl site densities, depending on the alumina(te) identity [54], we estimate their concentration to a range of roughly 0.1–2.0 OH/nm^2 on a typical alumina(te)-based catalyst support under tar reforming conditions at temperatures ≥800 °C. Quantitative K-titration of 0.1–2.0 OH/nm^2 would correspond to 8–163 μg K/m^2, to be compared to the 10–40 μg K/m^2, observed in our experiments on a Ni/$MgAl_2O_4$ catalyst.

The observed K profile, shown in Fig. 5, as well as the result displaying K reaching a stable value at the inlet of the catalytic bed in Fig. 4, indicates that the bed nearly reached its K saturation at the end of Period 1. According to calculations, 30 h of 1 ppmv KCl dosing, during Period 1, corresponds to a total K content of the same order as approximately two K saturation layers for the whole bed, neglecting effects related to the mobility of potassium. In the subsequent Period 2, adsorbed potassium was removed up to almost 1/3 of the bed, indicating significant K mobility. As illustrated in Fig. 5, there is an indication of anti-correlation between sulfur and potassium concentration in the catalytic bed, similar to the anti-correlation indicated by the bed inlet data in Fig. 4. This may be related to K-induced S—Ni bond weakening as described earlier. As opposed to Fig. 4, concentration numbers in Fig. 5 are presented as ppmw because the anti-correlation relation between S and K becomes clearer compared to expressing it with normalized S and K content. If both K and S concentrations in Fig. 5 were normalized by average BET surface area (13.7 ± 1.6 m^2/g) of samples taken at different axial bed distances, taking into account the standard deviation of the normalized S content, the sulfur profile along the bed appears uniform. Nevertheless, normalized K content retains more or less the same profile in the catalytic bed with or without normalization against BET data. This may possibly be related to faster diffusivity and higher mobility of K in catalyst pellets, as well as in the bed compared to S. Therefore, a change through the bed is more evident for K than S, as the partial pressure of dosing K changes in Period 2. While it is inconclusive as to whether an S and K anti-correlation exists in the bed, it is confirmed that K is transferred from 1/3 of the catalytic bed, due to no KCl dosing in Period 2. For the remaining part of the bed, K is in a similar equilibrium state as in the end of Period 1, due to the varying gas-phase KCl/KOH partial pressure in the bed as a result of the transport kinetics.

4.2. Effect of potassium on catalyst activity

In Fig. 6, methane, naphthalene and C_{10+} conversion increases over time as K uptake increases during Period 1 at higher rates in the beginning and with stabilized activities toward the end of the period, as K most likely reached equilibrium on the catalyst surface, as well as in the catalytic bed. The reason for improved reforming activity for both methane and tar may be related to K adsorption, lowering the surface coverage of S at active sites due to weakening of Ni—S bonds, as described earlier. Since S adsorbs stronger than K on Ni [39], it is a worse inhibitor and reducing its coverage gives a positive effect, improving the reforming performance of the catalyst.

Although in traditional steam reforming, K can retard the activity of the catalyst, due to blockage of the active Ni (step) sites [26], it appears in the present study to lower the surface S coverage (θ_s) at active Ni sites, increasing methane as well as tar reforming. This has been observed in other studies [55] [34] for CH_4 reforming. For instance, K promoted activation of methane on a K doped NiO/Ni(100) surface was observed by Chen et al. [55], relating the activity promotion to improved selectivity of NiO toward C—H cleavage [55]. Wangen et al. [34] investigated a reforming catalyst doped with KCl and KNO_3 and observed slight enhancement of the CH_4 reforming rates, although a severe deactivation was observed at higher concentrations. Similarly for tar reforming, Kuchonthara et al. [56] reported on improved steam reforming of tar in the presence of potassium. Alkali doping has also been shown to result in significantly increased reactivity of an inert (alumina) support surface toward tar molecules [57]. Another reason for the observed methane reforming improvement by time on stream is a less retarding effect of tar. It is known that the rate of catalyst poisoning increases with increasing boiling point of hydrocarbons [58]. Studies by Jess [59], revealed a retarding site blocking effect of naphthalene on methane reforming due to strong adsorption on the catalyst surface. There were no evidence of benzene affecting the conversion of methane. Wangen et al. [34] also observed the loss of CH_4 conversion in the presence of toluene, attributing the effect to competative adsorption of toluene and methane [34]. In a study by Dagle et al. [60], the effect of tar concentration and composition on catalyst steam reforming activity was investigated. The results showed that an increased concentration of tar significantly influenced the catalyst activity, with a more severe loss of activity in case of naphthalene (two C_6-ring aromatics), compared to benzene (one C_6-ring aromatics) [60]. Regarding the site blocking effect of tar on hydrocarbons other than methane, Jess [59] observed that naphthalene had a retarding effect on benzene. To the best of the author's knowledge, there are no other studies proving the same retarding effect of higher hydrocabons on other hydrocarbons than methane and benzene. Therefore, it is not conclusive to attribute this retarding effect of tar components on conversion of any other hydrocarbons except for methane and benzene.

Essentially carbon-free operation was established during the test, and thus no deactivation due to carbon formation is expected. The measured amount of carbon in the pretreated sample was 560 ppmw and the average C content over time on stream was around 3200 ppmw, staying stable over time. The average C content measured at the end of Period 2 (approximately 3700 ppmw) was also stable through the bed. Therefore, the promoting effect of K on methane and other hydrocarbons is not related to changes in carbon deposition.

As shown in Fig. 7, the observed decrease of methane conversion in Period 2 could be explained by the reverse phenomenon due to K adsorption in Period 1. The decrease in sulfur resistivity and consequently further passivation of catalyst and stronger bonds of S with Ni caused a lower methane conversion.

In case of naphthalene and C_{10+}, the conversion in Period 2 did not change after K removal as shown in Fig. 7. There is indication of average lower naphthalene conversion, but considering the standard deviations for the data, it is not statistically significant. The observed results may be related to methane being more intra-particle sensitive, compared to naphthalene and C_{10+}. In the previous study [45], during the transient activity period, naphthalene reached a stable condition, while methane conversion was still changing. This was concluded to be related to intra-particle diffusion restriction inside the catalyst for naphthalene being more severe than for methane [45]. This results in a lower utilization of the particle core for naphthalene reforming relative to methane

and, consequently, the S-equilibrated coverage is more quickly established in the volume utilized for naphthalene and methane reforming. Jess [59] and Aznar et al. [61] observed a selective deactivation due to H_2S, where methane reforming was hindered while tar reforming either maintained its activity or the decline in relative reaction rate for tar was less than for methane. Similarly, this may be the reason why methane conversion is more affected by potassium desorption than the higher hydrocarbons, in the present study. As K desorption occurs in period 2, the volume for established K-equilibrated coverage became smaller, affecting the methane conversion in a more significant way than conversion of higher hydrocarbons. This phenomenon has not been investigated for alkali species before. Another reason why conversion of higher hydrocarbons did change in Period 2 could be, as the K desorption front moves through the bed over time, fewer K-modified surface sites is available for methane and naphthalene conversion. This together with the fact that at high temperature, naphthalene is more easily reformed than methane at a catalyst surface [59], may explain that the fewer K-modified surface sites is still sufficient for the observed high conversions of naphthalene and other higher tar compounds.

5. Conclusion

Experimental studies have been carried out in order to establish the K coverage on a Ni-based tar reforming catalyst and its effect on the activity under real steady-state condition. K adsorption on the Ni catalyst reached almost equilibrium after 30 ToS with 1 ppm KCl dosing at 800 °C. This confirmed and extended the findings of our previous study on early stages of K adsorption and the indication of a slow approach to equilibrium. It can thus be concluded that relevant K equilibrium coverages on our $Ni/MgAl_2O_4$ steam reforming catalyst under real tar reforming conditions, which were previously unknown, are in the range of 10–40 μg K/m^2 BET. For typical Ni-based steam reforming catalysts under tar reforming conditions at temperatures ≥800 °C, we extrapolate relevant K equilibrium coverages to be below 100 μg/m^2. Although K is known to block active Ni sites and decrease the catalyst activity in traditional steam reforming, it appears to lower the surface S coverage (θ_S) at active Ni sites and increase methane as well as tar reforming in the present study. The reason appears to be a K-induced softening of the S—Ni bond and hence an increase in sulfur resistivity. The result is not solely conclusive and further investigation is needed to fully understand how sulfur adsorption is energetically influenced by relevant K coverages in a K-S/Ni system under reforming conditions. The K-modified support surface may also contribute to the increase in reactivity towards tar components.

The whole bed was close to reaching its K saturation point, according to the measured K profiles along the bed. During the K desorption period, the reforming of methane considerably decreased due to a reduction in sulfur resistivity while higher hydrocarbons conversion did not change significantly. This was discussed to be the result of intra-particle diffusion limitations being less severe for methane as well as well as the dynamics of the bed changing over time due to the K desorption front moving through the bed. Extended methane and tar reforming activity studies during the K desorption phase are needed for further insight, which may also shed more light onto the importance of the K-modified support surface reactivity toward tar molecules.

Acknowledgments

The Haldor Topsoe A/S chemical-analytical laboratory is gratefully acknowledged for LECO S and C analyses of catalyst samples. This work was carried out within the Swedish Gasification Center consortium. Funding from the Swedish Energy Agency, academic and industrial partners (E.ON and ANDRITZ) is gratefully acknowledged. The authors appreciate the contribution of Mr. Oumar Abdoulkarim in operating the gasification setup.

References

[1] F.L. Chan, A. Tanksale, Renewable Sustainable Energy Rev. 38 (2014) 428–438.
[2] P. McKendry, Bioresour. Technol. 83 (2002) 37–46.
[3] D. Dayton, A review of the literature on catalytic biomass tar destruction National Renewable Energy Laboratory (NREL), Colorado (2002).
[4] L. Devi, K.J. Ptasinski, F.J.J.G. Janssen, Biomass Bioenergy 24 (2003) 125–140.
[5] G. Berndes, M. Hoogwijk, R. van den Broek, Biomass Bioenergy 25 (2003) 1–28.
[6] E. Kurkela, M. Kurkela, I. Hiltunen, Fuel Process. Technol. 141 (2015) 148–158.
[7] A. Kumar, D.D. Jones, M.A. Hanna, Energies 2 (2009) 556–581.
[8] K. Salo, W. Mojtahedi, Biomass Bioenergy 15 (1998) 263–267.
[9] S.Q. Turn, Ind. Eng. Chem. Res. 46 (2007) 8928–8937.
[10] V. Nemanova, T. Nordgreen, K. Engvall, K. Sjöström, Catal. Today 176 (2011) 253–257.
[11] T.A. Milne, N. Abatzoglou, R.J. Evans, Biomass gasifier tars: their nature, formation, and conversion, Colorado (1998).
[12] J. Corella, A. Orio, J.M. Toledo, Energy Fuels 13 (1999) 702–709.
[13] Y. Shen, K. Yoshikawa, Renewable Sustainable Energy Rev. 21 (2013) 371–392.
[14] M.M. Yung, W.S. Jablonski, K.A. Magrini-Bair, Energy Fuels 23 (2009) 1874–1887.
[15] W. Torres, S.S. Pansare, J.G. Goodwin Jr., Catal. Rev. 49 (2007) 407–456.
[16] S. Anis, Z.A. Zainal, Renewable Sustainable Energy Rev. 15 (2011) 2355–2377.
[17] D. Sutton, B. Kelleher, J.R.H. Ross, Fuel Process. Technol. 73 (2001) 155–173.
[18] S.Q. Turn, C.M. Kinoshita, D.M. Ishimura, J. Zhou, Fuel 77 (1998) 135–146.
[19] H. Cui, S.Q. Turn, V. Keffer, D. Evans, T. Tran, M. Foley, Fuel 108 (2013) 1–12.
[20] E. Simeone, M. Siedlecki, M. Nacken, S. Heidenreich, W. de Jong, Fuel 108 (2013) 99–111.
[21] S. Tuomi, E. Kurkela, P. Simell, M. Reinikainen, Fuel 139 (2015) 220–231.
[22] W. Mojtahedi, M. Ylitalo, T. Maunula, J. Abbasian, Fuel Process. Technol. 45 (1995) 221–236.
[23] C. Erbel, M. Mayerhofer, P. Monkhouse, M. Gaderer, H. Spliethoff, Proc. Combust. Inst. 34 (2013) 2331–2338.
[24] H. Fatehi, Y. He, Z. Wang, Z.S. Li, X.S. Bai, M. Aldén, K.F. Cen, Proc. Combust. Inst. 35 (2014) 2389–2396.
[25] M. Wellinger, S. Biollaz, J. Wochele, C. Ludwig, Energy Fuels 25 (2011) 4163–4171.
[26] J.R. Rostrup-Nielsen, L.J. Christiansen, Concepts in Syngas Manufacture, Imperial College Press, London, 2011.
[27] I. Alstrup, B.S. Clausen, C. Olsen, R.H.H. Smits, J.R. Rostrup-Nielsen, Stud. Surf. Sci. Catal. 119 (1998) 5–14.
[28] J. Sehested, Catal. Today 111 (2006) 103–110.
[29] Y. Shigehara, A. Ozaki, J. Catal. 31 (1973) 309–312.
[30] J. Rostrupnielsen, J. Catal. 85 (1984) 31–43.
[31] C.H. Bartholomew, Appl. Catal. A: Gen. 212 (2001) 17–60.
[32] H.S. Bengaard, J.K. Nørskov, J. Sehested, B.S. Clausen, L.P. Nielsen, A.M. Molenbroek, J.R. Rostrup-Nielsen, J. Catal. 209 (2002) 365–384.
[33] J.R. Rostrup-Nielsen, P.E.H. Nielsen, Catalyst deactivation in synthetic gas production, and important syntheses, in: H. Wise, J. Oudar (Eds.), Catalyst Poisoning and Deactivation, Marcel Dekker New York, 1985, pp. 259–323.
[34] E.S. Wangen, A. Osatiashtiani, E.A. Blekkan, Top. Catal. 54 (2011) 960–966.
[35] I. Chen, D. Shiue, Ind. Eng. Chem. Res. 27 (1988) 1391–1396.
[36] A. Politano, V. Formoso, R.G. Agostino, E. Colavita, G. Chiarello, J. Chem. Phys. 128 (2008) 1–5.
[37] Z.P. Liu, P. Hu, J. Am. Chem. Soc. 123 (2001) 12596–12604.
[38] M. Ferrandon, J. Mawdsley, T. Krause, Appl. Catal. A: Gen. 342 (2008) 69–77.
[39] A.C. Papageorgopoulos, M. Kamaratos, J. Phys.: Condens. Matter 12 (2000) 9281–9291.
[40] M. Błaszczyszyn, Surf. Sci. 151 (1985) 351–360.
[41] M. Błaszczyszyn, M. Błaszczyszynowa, W. Gubernator, Acta Phys. Pol. A 88 (1995) 1151–1160.
[42] Y.P. Li, T.J. Wang, C.Z. Wu, Y. Gao, X.H. Zhang, C.G. Wang, M.Y. Ding, L.L. Ma, Ind. Eng. Chem. Res. 49 (2010) 3176–3183.
[43] J. Einvall, S. Albertazzi, C. Hulteberg, A. Malik, F. Basile, A.-C. Larsson, J. Brandin, M. Sanati, Energy Fuels 21 (2007) 2481–2488.
[44] S. Albertazzi, F. Basile, J. Brandin, J. Einvall, G. Fornasari, C. Hulteberg, M. Sanati, F. Trifiro, A. Vaccari, Biomass Bioenergy 32 (2008) 345–353.
[45] P.H. Moud, K.J. Andersson, R. Lanza, J.B.C. Pettersson, K. Engvall, Fuel 154 (2015) 95–106.
[46] C. Brage, Q. Yu, G. Chen, K. Sjöström, Fuel 76 (1997) 137–142.
[47] S. Gordon, B.J. McBride, Computer Program for Calculation of Complex Chemical Equilibrium Compositions and Applications I. Analysis, 311, NASA reference publication, 1994.
[48] I. Alstrup, J.R. Rostrup-Nielsen, S. Røen, Appl. Catal. 1 (1981) 303–314.
[49] V. Nemanova, K. Engvall, Energy Fuels 28 (2014) 7494–7500.
[50] A. Iordan, M. Zaki, C. Kappenstein, J. Chem. Soc. Faraday Trans. 89 (1993) 2527–2536.
[51] Z. Zhang, Y. Zhang, Z. Wang, X. Gao, J. Catal. 271 (2010) 12–21.
[52] M. Digne, P. Sautet, P. Raybaud, P. Euzen, H. Toulhoat, J. Catal. 211 (2002) 1–5.
[53] H. Knözinger, P. Ratnasamy, Catal. Rev. 17 (1978) 31–70.

[54] J.I. Di Cosimo, M. Dıíez, E. Iglesia, C.R. Apesteguıía, J. Catal. 178 (1998) 499–510.
[55] J.G. Chen, M.D. Weisel, J.H. Hardenbergh, F.M. Hoffmann, C.a. Mims, R.B. Hall, J. Vac. Sci. Technol. A 9 (1991) 1684–1687.
[56] P. Kuchonthara, B. Puttasawat, P. Piumsomboon, L. Mekasut, T. Vitidsant, Korean J. Chem. Eng. 29 (2012) 1525–1530.
[57] L.K. Mudge, E.G. Baker, D.H. Mitchell, M.D. Brown, J. Sol. Energy Eng. 107 (1985) 88.
[58] F. Moseley, R.W. Stephens, K.D. Stewart, J. Wood, J. Catal. 24 (1972) 18–39.
[59] A. Jess, Chem. Eng. Process. 35 (1996) 487–494.
[60] V.L. Dagle, R. Dagle, L. Kovarik, A. Genc, Y.-G. Wang, M. Bowden, H. Wan, M. Flake, V.-A. Glezakou, D.L. King, R. Rousseau, Appl. Catal. B: Environ. 184 (2016) 142–152.
[61] M.P. Aznar, M.A. Caballero, J. Gil, Ind. Eng. Chem. Res. 5885 (1998) 2668–2680.